C_{48} Buckybowl and C_{60} Fullerene Precursors on the Basis of Truxenone

Konstantin Yu. Amsharov and Martin Jansen

Max Planck Institute for Solid State Research, Heisenbergstrasse 1, 70569 Stuttgart, Germany

Reprint requests to Prof. M. Jansen. Fax: (+)497116891502. E-mail: m.jansen@fkf.mpg.de

Z. Naturforsch. **2007**, *62b,* 1497 – 1508; received July 27, 2007

The synthesis of bromine-substituted truxenone derivatives which constitute prospective precursors of geodesic structures is presented. The underlying mechanism of fullerene formation from truxenone-based precursors during flash pyrolysis is discussed. Isolable quantities of C_{60} fullerene have been achieved by intramolecular condensation of a precursor containing all 60 carbon atoms in appropriate positions, 72 out of the 90 required C–C bonds, and 3 bromine atoms.

Key words: Fullerene, Truxenes, Flash Pyrolysis, Cyclization

Introduction

The discovery of fullerenes has given rise to appreciable interest in the field of direct synthesis of fullerenes and non-planar "aromatic" structures which in principle can be regarded as fragments of the fullerene "surface". Research on geodesic structures potentially provides better understanding of the unique nature of fullerene properties that are a consequence of the non-planar π system. The synthesis methodology of geodesic structures can be successively applied to the synthesis of fullerenes. Direct synthesis is of great interest from both theoretical and practical points of view, in particular as a promising method for the synthesis of fullerenes which cannot be obtained during the uncontrolled process of graphite vaporization in an arc discharge.

As it was shown previously, many geodesic polyarenes can be obtained by intramolecular C_{Aryl}-C_{Aryl} condensation of polynuclear aromatic hydrocarbons (PAH), with the required location of all carbon atoms given, under flash vacuum pyrolysis (FVP) conditions. Representative results have been reported elsewhere [1 – 4]. As it was shown, the existence of a halogen atom in the initial precursor increases the yield of the desired product significantly. In some cases PAH analogs do not undergo intramolecular cyclization because during pyrolysis the carbon–halogen bond breaks homolytically more easily than the C–H bond. Typically, chlorine or bromine substituents are used for radical creation. The radical formed attacks the neighboring carbon atom, and the required bond is established. The C_{Aryl}–Br bond breaks more easily than the C_{Aryl}–Cl bond and the homolytic cleavage of the C_{Aryl}–Br bond occurs at temperatures lower than 900 °C [5, 6]. If the formation of a new C–C bond with a carbon atom bearing a radical is not possible due to geometrical constraints, a 1,2-shift of hydrogen is possible, thus leading to a displacement of the radical position [7]. Despite of the formally "incorrect" position of the halogen atom in the precursor, the following intramolecular condensation leads to the formation of the desired C–C bond. The mechanism of this process is presented in Fig. 1 for the example of the hemifullerene $C_{30}H_{12}$ (**II**) synthesis from the precursor **I** [8]. It is important to note that during the FVP process the corresponding bromine-free precursor does not yield the desired product [9].

This methodology was successfully employed by Scott *et. al*. for C_{60} fullerene synthesis [10]. The pyrolysis precursor, containing all 60 carbon atoms at the desired positions, and three chlorine atoms for radical generation, was obtained through an 11-step synthesis. After the FVP of this precursor, C_{60} was obtained with 0.1 – 1 % yield. Despite of the relatively low yields, the high selectivity (formation of other fullerenes was not discernible) makes this approach very promising. Formation of C_{60} from a hydrocarbon analog which does not contain chlorine was observed only during high laser fluence in a LDI experiment [11]. Several synthetic strategies have been proposed for C_3-symmetrical C_{60} precursor synthesis [12 – 14]. However, the introduction of a halogen atom into the precursor structure remains a difficult experimental task, in all suggested routes.

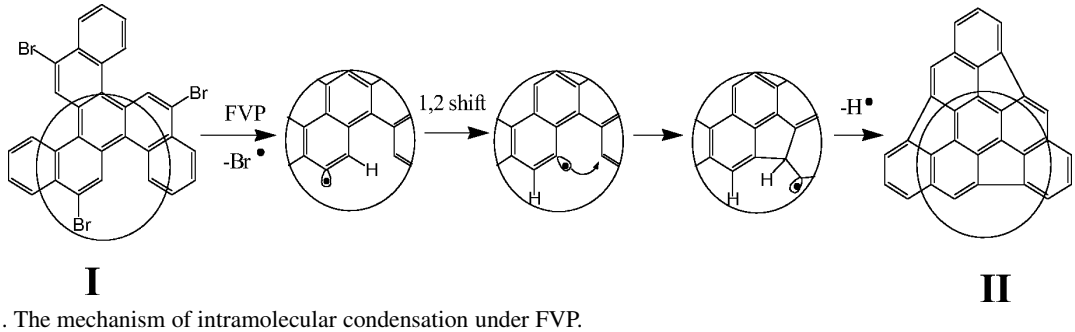

Fig. 1. The mechanism of intramolecular condensation under FVP.

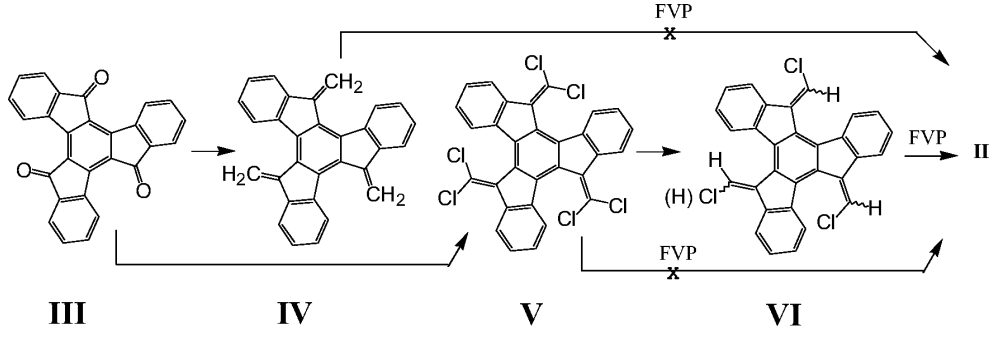

Fig. 2. Synthesis of hemifullerene **II** from a truxenone-based precursor.

Keeping in mind all stated above, we have chosen truxenone (**III**) as a starting unit. C_{48} buckybowl and C_{60} precursors containing all carbon atoms in the desired positions can be synthesized from truxenone in just two steps. Moreover, the scheme of synthesis has some advantages, especially in the case of halogen-containing precursors. The carbonyl group permits a selective Grignard addition without involving C_{Aryl}-halogen bonds. Thus, the halogen atom can be included either in a truxenone moiety or in the radical to be attached, or in both fragments at the same time.

The potential of truxene derivatives for the synthesis of buckybowl $C_{30}H_{12}$ (**II**) has been demonstrated by Rabideau *et al*. [15]. Pyrolysis of the truxene derivative **VI** (a mixture of trichloro and tetrachloro compounds) led to the desired product **II** with 10 – 15 % yield, while pyrolysis of compound **V** containing six chlorine atoms resulted in a complex mixture of chlorinated products [15]. Attempts of synthesizing hemifullerene **II** by pyrolysis of analogous PAH **IV** (Fig. 2) failed as well [16].

Later, Dehmol *et al*. [17] and Plater *et al*. [18] have independently synthesized triphenyltruxenene $C_{48}H_{30}$ (**VIIc**) which may serve as a precursor for the C_{48} fullerene fragment, the so-called deep-bowl structure representing 80 % of the C_{60} "surface". All attempts to achieve intramolecular condensation by melting together with $AlCl_3$/NaCl, heating with Pd/C, photochemical cyclization, and direct pyrolysis were unsuccessful. The analysis of the pyrolysis products showed the presence of low molecular mass products of decomposition exclusively [17].

Thus, one can conclude that bromine-containing truxenone derivatives are prospective pyrolysis precursors for a number of buckybowl structures as well as for fullerene cages. In this work we report on the synthesis of a number of bromine-substituted tribenzenetruxenes, pyrolysis precursors for the C_{48} buckybowl structure, and C_{60} fullerene pyrolysis precursors, on the basis of truxenone. The process of intramolecular condensation of PAH precursors as well as bromine-substituted analog under FVP condition was investigated. The mechanism of the precursors' intramolecular cyclization and fullerene formation under FVP conditions is discussed.

Results and Discussion

The structures of all precursors synthesized are compiled in Fig. 3. A mixture of *E/Z* isomers was the final product in all cases (**VIIc**, **VIIIc**, **IXc**, **Xc**, **XIc**).

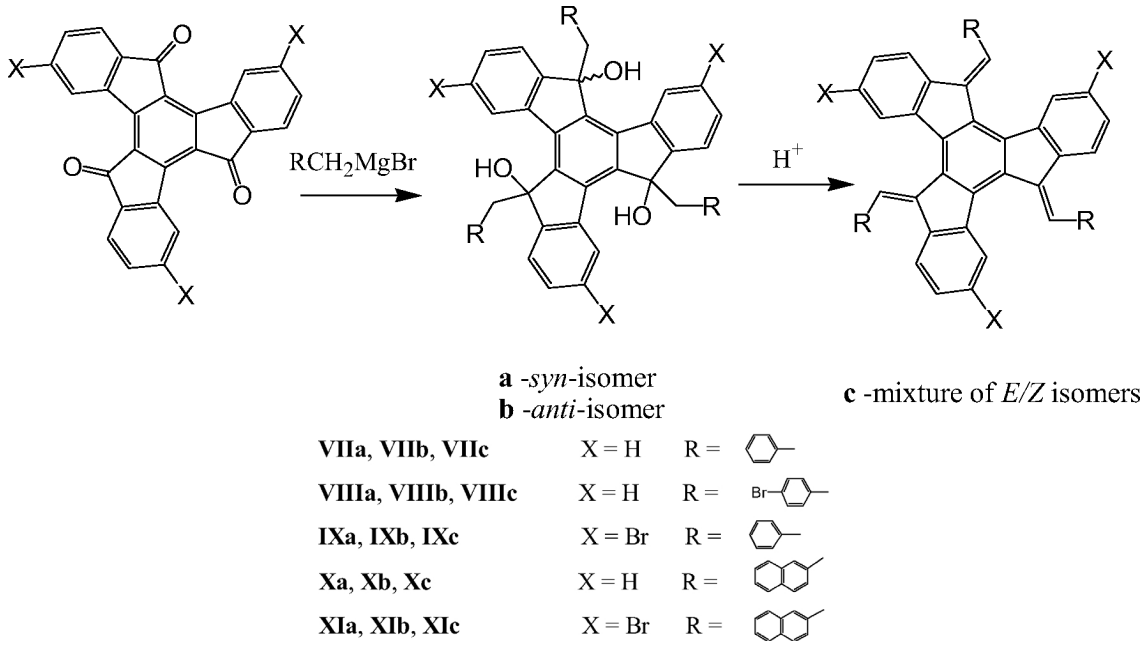

Fig. 3. Synthesis of C_{60} and C_{48} pyrolysis precursors on the basis of truxenone.

HPLC analyses of **VIIc** and **Xc** revealed the presence of three main isomers. It was found that the isomers undergo interconversion. Thus, separated individual isomers in toluene re-equilibrate into a mixture of three isomers within two days, the ratio of the isomers being equal to that in the initial mixture. Presence of *E/Z* isomers in the pyrolysis experiment did not affect the results, because at high temperatures the *E/Z* isomers equilibrate quickly.

Triphenyl- and trinaphthyl-substituted truxenenes (**VIIc**, **Xc**) are rather thermostable and can be easily transferred into the gas phase even in moderate vacuum (2 – 10 mbar). In the case of bromine-substituted analogs, especially the 3,8,13-tribromo derivatives (**IXc**, **XIc**), significant destruction of the initial compound takes place. Nevertheless, under high-vacuum conditions ($10^{-3} – 10^{-4}$ mbar) it is possible to transfer most of the precursor into the gas phase. It was discovered that pyrolysis at 1000 °C of triphenyl- as well as of trinaphthyl-truxenenes leads to the formation of fullerenes C_{60} and C_{70} and a number of higher fullerenes, according to LDI MS data. The formation of C_{60} from the C_{48} buckybowl precursor as well as the formation of higher fullerenes from the C_{60} precursor show that under the given conditions the mechanism of fullerene assemblage is not a result of intramolecular condensation, or is at least complicated by various parallel processes. On the other hand, it was shown that the pyrolysis at 900 °C results in products of intramolecular condensation only. For studying the mechanism of condensation, pyrolysis experiments were performed at this lower temperature, which allowed the exclusion of most of the side processes.

C_{48} buckybowl precursors

Taking into account that the pyrolysis process can be complicated by spontaneous fullerene formation, we have chosen tribenzyltruxenes – precursors of the C_{48} buckybowl (carbon backbone presented in Fig. 7) – as a model for investigating the intramolecular condensation under FVP conditions. The degree of condensation during FVP can be easily determined from the MS data. The presence of C_{60} signals clearly points to "non-direct" fullerene formation under the given conditions.

LDI analysis of the products obtained after pyrolysis of tribenzylidenetruxene (**VIIc**) and its brominated analogs (**VIIIc, IXc**) showed four main groups of signals in the mass spectrum in the range of m/z = 500 – 600, minor amounts of products of dimerization in the range of m/z = 900 – 1050 and no signals of fullerene clusters (Fig. 4). The group of signals number 4 corresponds to the initial tribenzyltruxene and the products

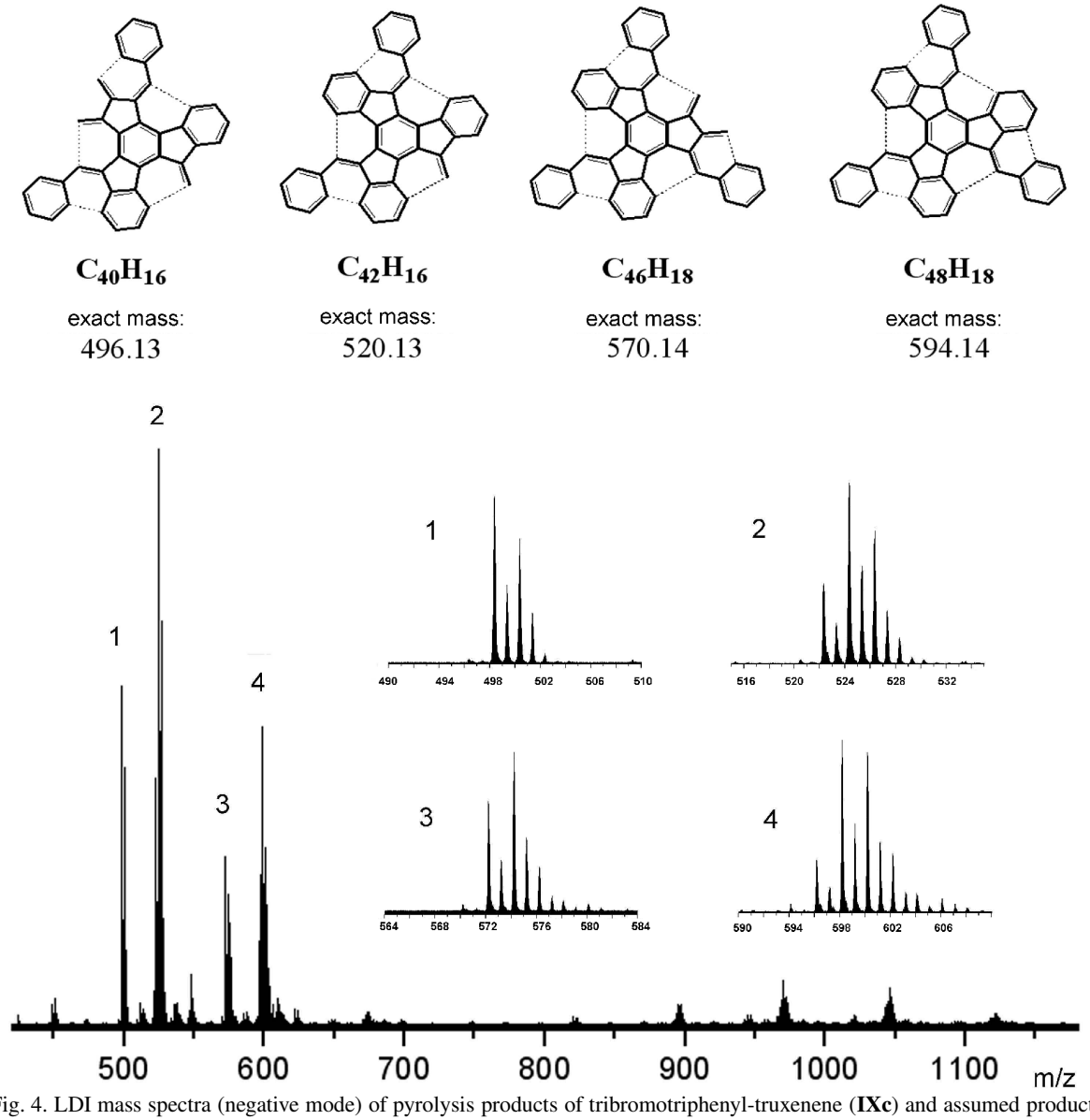

Fig. 4. LDI mass spectra (negative mode) of pyrolysis products of tribromotriphenyl-truxenene (**IXc**) and assumed products of intramolecular cyclization.

of its intramolecular condensation accompanied by the loss of n hydrogen molecules ($M' = M - 2n$ Da). The lowest mass detected in this group is 594.2 Da and corresponds to $C_{48}H_{18}$ which is the result of eliminating 12 hydrogen atoms and generating of 6 new C–C bonds in the initial precursor. The groups of signals 1, 2 and 3 correspond to the products of partial fragmentation of the precursor. The second group of signals indicates loss of a phenyl ring yielding $C_{42}H_{24}$ ($m/z = 528.2$), the intramolecular condensation of which gives $C_{42}H_{22}$, $C_{42}H_{20}$ and $C_{42}H_{18}$, respectively, and $C_{42}H_{16}$ as the product of maximal condensation ($m/z = 520.2$). In the same way the group 3 of signals corresponds to the loss of a C_2 fragment and formation of products of the consecutive cyclization. The group 1 of signals indicates loss of a phenyl and of a C_2 fragment at the same time. The molecular structures assigned to the products with maximal degree of condensation are shown

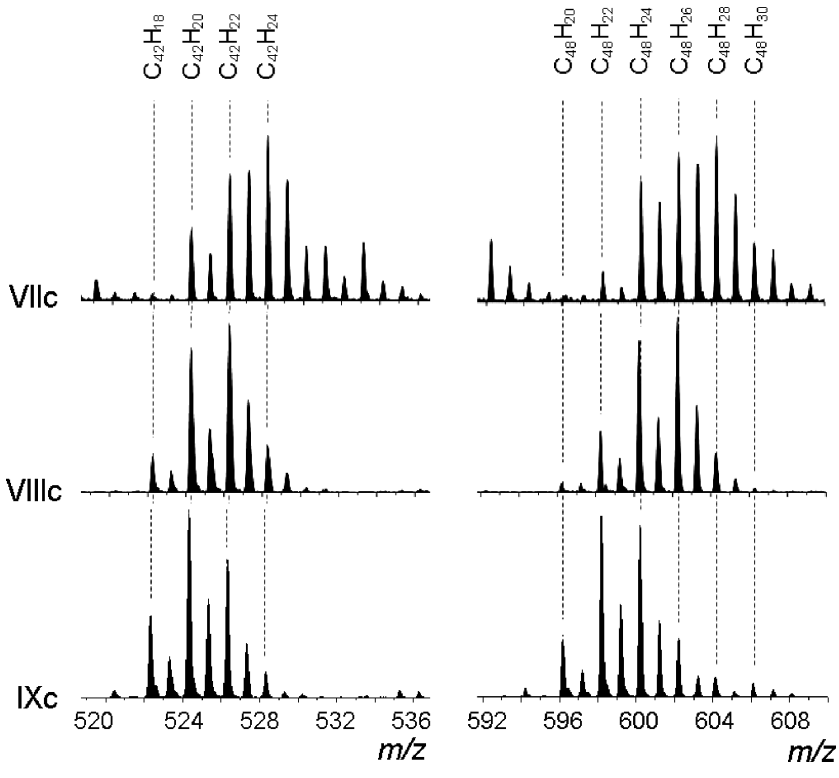

Fig. 5. LDI mass spectra of pyrolysis products of **VIIc**, **VIIIc** and **IXc**.

in Fig. 4. Newly formed C–C bonds are presented by dotted lines.

Through intramolecular condensation triphenyltruxenene can theoretically form 9 new bonds (Fig. 7). The product with the maximal degree of condensation which was observed in the LDI experiment ($C_{48}H_{18}$) has only 6 new bonds. The structure of $C_{48}H_{18}$, as well as those of $C_{46}H_{18}$, $C_{42}H_{16}$ and $C_{40}H_{16}$, can be represented by a number of structural isomers. However, a detailed analysis of the products of the partial fragmentation leads to the structures proposed in Fig. 4. It is obvious that the loss of a phenyl group results in one bond less than the number of new C–C bonds in the product with the highest degree of condensation ($C_{42}H_{16}$). This gives evidence for a phenyl fragment possessing only one additional bond with the truxene core in $C_{48}H_{18}$. On the other hand, loss of a C_2 fragment is possible only for the terminal benzene ring of the truxene fragment (atoms C2–C3, C7–C8 or C12–C13; for numeration of truxene atoms see Fig. 7). This implies the formation of additional bonds with the truxene core through C1, C6 and C11 carbon atoms. Another possible way of bond formation between the phenyl fragments and the C3, C8 and C13 atoms, with subsequent elimination of C_2 fragments (atoms C1–C2, C6–C7 and C11–C12), leads to a less probable structure containing five-membered cycles at the periphery of the molecule.

In the case of triphenyltruxenene (**VIIc**) pyrolysis, the mass spectrum is more complex than those of the bromine-containing compounds (**VIIIc** and **IXc**). However, one can again clearly see all four groups of signals. The products of pyrolysis contain the initial precursor $C_{48}H_{30}$ as well as the products of condensation: $C_{48}H_{28}$, $C_{48}H_{26}$ and $C_{48}H_{24}$. Signals of products of further condensation are either very weak or completely absent. In several independent experiments the product ratios varied significantly. Yet, in all cases the most intense signals corresponded either to the initial precursor or to one of the three condensation products ($C_{48}H_{28-24}$). In some experiments a weak signal of $C_{48}H_{22}$ was observed (Fig. 5).

Pyrolysis of phenyltruxenene containing a bromine atom in *para* position of the phenyl ring showed better reproducibility. In the corresponding mass spectra of the products of pyrolysis the signal of the initial precursor had almost vanished and a relatively intense signal of $C_{48}H_{22}$ was observed (Fig. 5). The most

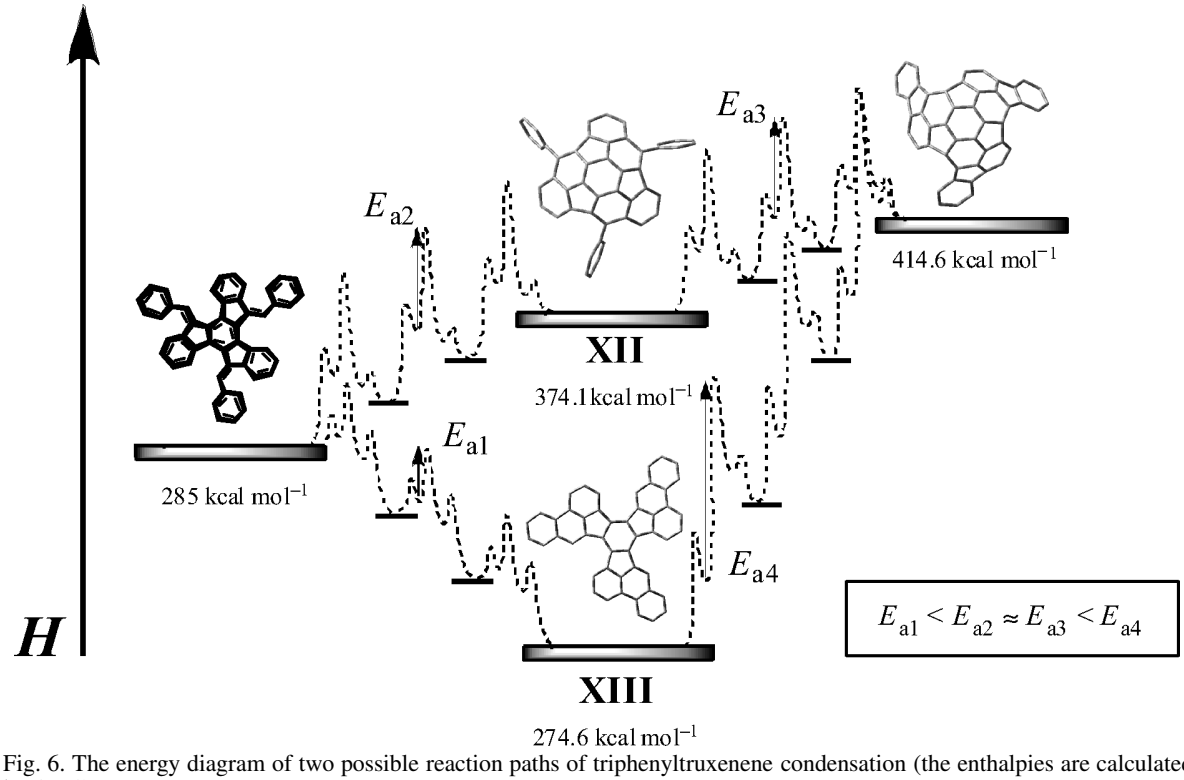

Fig. 6. The energy diagram of two possible reaction paths of triphenyltruxenene condensation (the enthalpies are calculated by AM1).

prominent signals were always those of $C_{48}H_{26}$ and $C_{48}H_{24}$.

Pyrolysis of the bromine-substituted phenyltruxenene **IXc** showed very good reproducibility. Virtually identical spectra were obtained by MS analysis in five independent experiments both in the positive and negative modes. In addition to the signal of $C_{48}H_{24}$, intense signals of products of higher condensation $C_{48}H_{22}$ and $C_{48}H_{20}$ were observed, as well as weak signals of $C_{48}H_{18}$ (Fig. 5). The same regularities were observed for the products of fragmentation. As it can be seen from Fig. 5, pyrolysis of **IXc** gives a C_{42}-PAH with a high degree of condensation ($C_{42}H_{18}$). The signals of $C_{42}H_{24}$ dominate in the pyrolysis products of the hydrocarbon analog **VIIc**, which corresponds to the formation of only one new C–C bond.

In summarizing, the products of the triphenyltruxenene (**VIIc**) pyrolysis contain the major part of the initial precursor and the cyclization process stops after formation of three new bonds. Introduction of bromine into the *para* position of the phenyl ring (**VIIIc**) significantly increases the efficiency of the condensation, and signals of the initial precursor are no longer detectable in the spectra. Nevertheless, the process of condensation stops after the formation of three new bonds, and only minor amounts of products of higher condensation are present. Mass spectra of the products of the tribromotriphenyltruxene **IXc** pyrolysis show a higher degree of condensation of the precursor. This difference can be explained by the different possible ways of reaction leading to highly condensed structures. In Fig. 6 two possible reaction paths of buckybowl $C_{48}H_{18}$ formation are schematically shown. As it can be seen, changing the condensation sequence results in different reaction profiles (both profiles presented are borderline cases; other combinations of condensations have intermediate energy values).

Activation energies for each step can be estimated from the difference of enthalpy of reaction according to the Bell-Evans-Polanyi principle ($E_a = A + B\Delta H_r$), since all elementary steps of condensation are closely related reactions. The rate of each condensation will be determined by the difference between the heat of formation of the educt and the product of the rate-determining step. As one can see from the reaction mechanism (Fig. 1), the cyclization process consists

of three elemental stages, the second of which (intramolecular radical attack) being the rate-determining one. We do not exclude the possibility of high activation barrier values for the first step in the case of hydrocarbon analogs, which can influence significantly the kinetics of the whole process. During processes involving bromine radicals the "loss" of a proton is associated with a low activation barrier [19].

It is clear from Fig. 6 that in the case of triphenyltruxenene pyrolysis the formation of a stable and almost planar structure **XIII** is energetically the most favorable. The activation energy of the rate-determining step (E_{a1}) is low for this process. The corresponding enthalpy change (ΔH_r) is about 40 kcal mol^{-1}. Further cyclization of compound **XIII** requires a significantly higher activation energy, E_{a4} (ΔH_r = 3 – 4 kcal/mol). Therefore, the probability of this process to take place is low.

During the pyrolysis of precursor **VIIIc**, containing bromine atoms, many radicals can be formed, thus stimulating the precursor condensation. Nevertheless, no big changes during pyrolysis are observed because of "wrong" positions of bromine atoms in the precursor. The initial precursor is present in minor amounts among the pyrolysis products. Compounds corresponding to a higher condensation are present as well, but in general the condensation process stops after the formation of the stable structure **XIII** (Fig. 6). Minor differences between the composition of pyrolysis products of **VIIIc**, possessing bromine atoms at "wrong" positions, and the pyrolysis products of the hydrocarbon analogue **VIIc** confirm our assumption that the second step of the reaction (intramolecular radical attack) determines the kinetics of the whole process.

In the case of triphenyltruxenene **IXc**, which has three bromine atoms in positions 3, 8 and 13 in the truxene core (numbering is shown in Fig. 7), homolytic cleavage of the C–Br bond leads to formation of radicals in the corresponding positions. Three subsequent 1,2-hydrogen shifts result in relocation of the radicals to positions 4, 9 and 14. The following cyclization leads to compound **XII**. The activation energy (E_{a2}) of this process is rather low (ΔH_r = 30 kcal mol^{-1}). The subsequent cyclization of compound **XII** requires significantly lower activation energy (E_{a3}, ΔH_r = 25 kcal mol^{-1}) than in the case of compound **XIII** (E_{a4}, ΔH_r = 37 – 40 kcal mol^{-1}). As a result, the condensation process takes place, and highly condensed products are formed. Thus, introduction of bromine atoms at specific sites leads to changes in the path of buckybowl $C_{48}H_{18}$ formation. This path does not possess any deep energy minimum, and results in a high degree of intramolecular condensation.

C_{60} fullerene precursors

As one can see from Fig. 7, the naphthyl-substituted truxenene represents a C_{60}-related structure that contains all 60 carbon atoms in the required positions for building the C_{60} fullerene molecule. This structure contains 72 of 90 C–C bonds, which corresponds to 80 % of all bonds in C_{60}. The structural similarity between C_{48} and C_{60} precursors allows one to transfer the systematics found for triphenyltruxenene to trinaphthyltruxenene. Namely, the introduction of bromine atoms at positions 3, 8 and 13 of trinaphthyltruxenene should also promote a high degree of condensation during the FVP process. In order to verify this suggestion, both trinaphthyltruxenene (**Xc**) and its 3, 8, 13-tribromo analog (**XIc**) were synthesized and investigated as pyrolysis precursors of C_{60}.

The mass spectrum of the pyrolysis products of **Xc** in the positive mode was very complex (Fig. 8a). Despite the difficulties in analyzing the spectrum because of the large number of signals, some groups can be clearly distinguished, *i. e.* signals corresponding to the initial precursor (*m/z* = 756.3) and to the products of its intramolecular condensation, as well as signals corresponding to the loss of one naphthalene molecule (*m/z* = 628.2). Although no C_{60} signals could be observed in the positive mode, the mass spectrum of this sample in the negative mode clearly showed the presence of C_{60} fullerene (Fig. 8b). Such a big difference between the spectra in positive and negative modes can be explained by the easy formation of the fulleride anion. This permits the detection of even trace amounts of fullerene in the sample. Despite the minor amounts

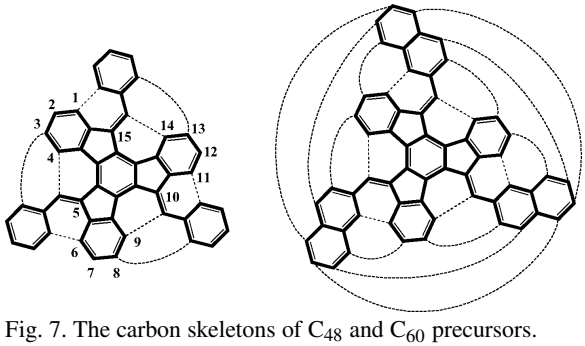

Fig. 7. The carbon skeletons of C_{48} and C_{60} precursors.

of C_{60} in the sample, the presence of fullerene C_{60} after pyrolysis of the C_{60} precursor (Fig. 8) and its absence after pyrolysis of the C_{48} precursor (Fig. 4) confirm the mechanism of fullerene formation *via* intramolecular condensation.

The analysis of the pyrolysis products of the tribromo-substituted analog (**XIc**) showed an intense signal corresponding to fullerene C_{60}, observed in both negative and positive modes (Fig. 8c). Fast sublimation of compound **XIc** during pyrolysis allowed identification of the intermediate products of condensation. In the mass spectrum of the obtained sample the sequences observed for triphenyltruxenenes were also clearly seen (Fig. 8d). Thus, the most intense group of signals corresponds to a fragment C_{50}, which indicates the elimination of one naphthalene molecule. Analysis of highly condensed products of this group reveals the formation of up to eight new bonds ($C_{50}H_{14}$), which is in good agreement with the proposed structure. The signals in the region of m/z = 634 – 640 may be related to the C_{52} structures. In the range of m/z = 740 – 750 signals corresponding to products of intramolecular condensation of the initial precursor are observed. The structure $C_{60}H_{20}$, which has the highest degree of condensation, corresponds to the formation of 8 new bonds in the initial precursor. The structure with the lowest degree of condensation observed in the spectrum is $C_{60}H_{30}$. It corresponds to the formation of 3 new bonds, thus being also in good agreement with the proposed mechanism.

We did not detect signals of intermediate products in the range $C_{60}H_{18}$–$C_{60}H_2$. According to the MS data, the intramolecular condensation was over after formation of the $C_{60}H_{20}$ structure in all cases. The next intense m/z signal corresponds to fullerene C_{60}. We explain this by the spontaneous collapse of $C_{60}H_{18}$ with the formation of the fullerene molecule because of the kinetic instability of intermediate products.

The mechanism of fullerene formation

It is logical to assume that the most closely placed carbon atoms are able to form a new bond. Such a cyclization reduces the distance between the next pair of carbon atoms and the process of condensation proceeds step by step. The so called "zipper" mechanism of fullerene formation takes place. Calculations of the enthalpies of formation of the intermediate products in the range $C_{60}H_{30}$–C_{60} show that every subsequent condensation is getting energetically less favorable and

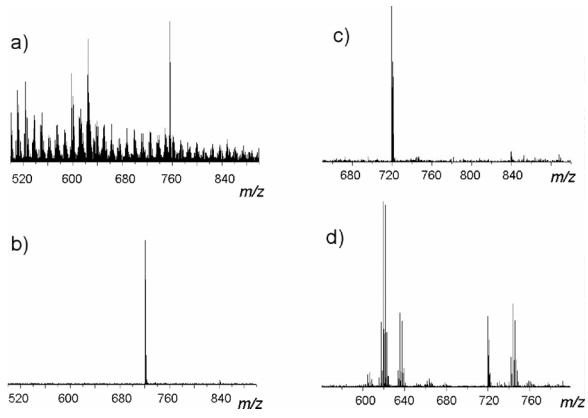

Fig. 8. LDI mass spectra of pyrolysis products: a) **Xc**, positive mode; b) **Xc**, negative mode; c) **XIc**, positive mode; d) **XIc**, negative mode (fast sublimation of the precursor).

only for the steps $C_{60}H_{12}$–$C_{60}H_6$ a minor reduction of ΔH_r is observed [20]. Hence, the intermediate products should be relatively stable. A comparison of the stabilities on the basis of calculated energies of formation witnesses that such open structures can exist [21]. The activation energies (as estimated from reaction enthalpies of the rate-determining stages) do neither explain the absence of intermediate products $C_{60}H_{18}$–$C_{60}H_2$ during the condensation. We believe that the heat of formation can not be used for the estimation of stabilities in this case because significant changes in the carbon skeleton do not permit to consider the later stage condensation processes as closely related reactions. In other words, the rate of cyclization at later stages ($C_{60}H_{20}$–C_{60}) does not correlate with the heats of formation.

Taking into account the cyclization mechanism and the geometry of the molecule, one might assume that decreasing the carbon-carbon distance would lower the energetic barrier of the bond formation between these carbon atoms: as the geometry of the starting conformation gets closer to the geometry of the transition state, according to Hammond's postulate, the activation energy of a process decreases. Therefore, the variation of C–C distances at first approximation can be used as a comparative estimate of the activation energy for each condensation stage.

The evolution of the distance between the two most closely placed carbon atoms during condensation is presented in Fig. 9. During the first condensation steps, the molecules are not rigid and some fragments possess conformational mobility. The minimal possible distance in this case is determined by the van-der-Waals

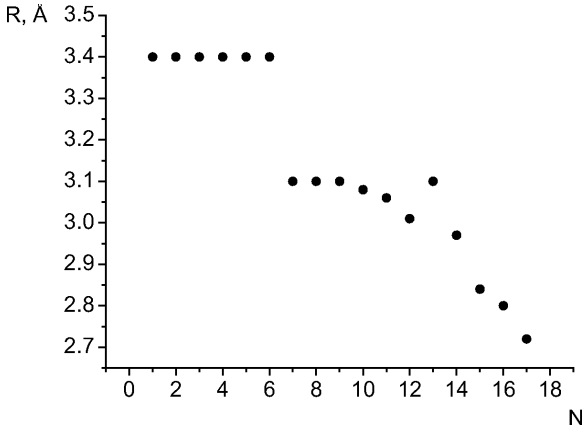

Fig. 9. Dependence of the C–C distance (*R*) on the number of condensation stages in the course of the intramolecular condensation of trinaphthyltruxenene (optimized by PM3).

radius of carbon (1.7 Å). At a certain stage of the condensation, the molecules lose conformational mobility. Non-planar geometry causes a significant shortening of the distances between peripheral carbon atoms. After the 7th condensation step the minimal C–C distance is 3.1 Å which is less than two carbon van-der-Waals radii. Each following condensation step leads to a further decrease in the respective C–C distance. At a threshold value, the activation barrier becomes so low that the simultaneous formation of all still missing C–C bonds of C_{60} becomes possible. As a result the "collapse" of the structure takes place and a fullerene molecule is formed, in virtually one final step.

The yield of fullerene under low-temperature pyrolysis conditions (900 °C) of **XIc** is 0.01 – 0.05 % according to HPLC data. Increasing the temperature up to 1000 °C leads to a higher yield of fullerene of about 0.5 %. Taking into account the partial fragmentation of the precursor (by the cleavage of the bond between the naphthalene and truxenene units), the regioselectivity of the intramolecular condensation seems very high. It is possible that at high-temperature pyrolysis (1000 °C) some parallel processes take place which lead to fullerene formation as well. The presence of a trace amount of C_{70} fullerene in the pyrolysis products confirms this supposition. However, it is known that pyrolysis of aromatic hydrocarbons at such temperatures leads to fullerene formation only in trace amounts [22]. Thus, such high yields confirm that the main share of the fullerene yield is a result of direct intramolecular condensation of the precursor.

Conclusion

It has been shown that the truxenone molecule is a promising starting agent for the synthesis of halogenated precursors suitable for the generation of buckybowl and closed carbon structures through pyrolysis. The synthetic route proposed allows us to synthesize C_{60} related structures in two steps from commercially available reagents.

Bromine atoms activate the intramolecular condensation, while their positions determine the whole consecutive condensation process. Purposeful introduction of halogen atoms permits to direct the process in the desired direction to achieve high conversion.

Low temperature pyrolysis (900 °C) is not complicated by parallel processes which has allowed us to investigate the mechanism of precursor condensation in detail. The mechanism proposed includes step by step condensation during the first reaction stages (zipper mechanism). At a specific condensation stage, C_{60} formation takes place virtually in a single step as a consequence of quasi-simultaneous formation of all remaining bonds required for cage closure.

High yields of fullerene were achieved during intramolecular condensation of precursor **XIc** containing all 60 carbon atoms in the appropriate positions, 72 of 90 required C–C bonds and 3 bromine atoms. The relatively high and selective conversion makes such an approach very promising, especially concerning fullerenes which can not be obtained by the uncontrolled graphite evaporation technique.

Experimental Section

General methods and materials

The NMR spectra were recorded at 20 °C. R_f data were determinated on TLC-PET sheets coated with silica gel with a fluorescence indicator at 254 nm (layer thickness 0.25 mm, medium pore diameter 60 Å, Fluka). The MALDI-TOF MS spectra were obtained by using DCTB (*trans*-2-[3-(4-*tert*-butylphenyl)-2-methyl-2-propenylidene]malononitrile) or a mixture of DCTB with silver triflate as the matrix (Reflex IV, Bruker Daltonik GmbH, Bremen, Germany). Elemental analyses were performed on the Elemental Analyzer VARIO EL (Elementar, Hanau, Germany). HPLC analyses were carried out on a reverse phase column, Supelcosil LC-18-DB, size 4.6 × 250 mm, with a mobile phase of toluene : methanol (1 : 1), flow rate 1 mL min^{-1}, UV detection. Chromatographic purifications were carried out with flash grade silica gel Kieselgel 60 (0.06 – 0.2 mm, Roth). Quantum mechanical calculations were carried out using GAUSSIAN 03 [23]. Truxenone (diindeno[1,2-

a;1′,2′-c]fluorene-5,10,15-trione) [17] and 4,9,14-tribromotruxenone (3,8,13-tribromo-diindeno[1,2-a;1′,2′-c]fluorene-5,10,15-trione) [24] were prepared according to the described procedures. Details of the pyrolysis apparatus are reported elsewhere [25]. In a typical experiment, 5 – 10 mg of the sample was pyrolyzed. The resulting products were extracted with toluene in an ultrasonic bath. Extracts were filtered through microfilters (0.2 μm) and analyzed by LDI-TOF MS and HPLC.

Condensation of truxenone with Grignard reagent

2 mmol (769 mg) of truxenone was suspended in 15 mL of absolute diethyl ether in an ultrasonic bath. The suspension obtained was added to 10 mmol of the corresponding freshly prepared Grignard reagent in 10 – 20 mL of ether. The resulting mixture was refluxed for 2 – 3 h under constant stirring, cooled to r. t. and hydrolyzed by addition of NH_4Cl solution. The product was extracted with diethyl ether and dried over Na_2SO_4. The solvent was removed and the residue was chromatographicaly purified (silicagel, dichloromethane, DCM). After the elution of the *anti* isomer the mobile phase was changed to DCM acetone (20 : 1). After evaporation, the products were dissolved in small amounts of DCM and precipitated by addition of petroleum ether. The products were washed with petroleum ether and dried. The overall yield (both isomers) was about 40 – 60 %.

In the case of the 3,8,13-tribromo derivatives, 2 mmol of the Grignard reagent and 0.3 mmol of tribromotruxenone were used. Separation and purification were carried out using the same method.

Truxenetriol dehydrogenation

The *syn* or *anti* isomer or their mixture (0.2 – 0.5 g) was dissolved in a small amount of acetic acid. After addition of a catalytic amount of H_2SO_4 the mixture was refluxed at 110 °C with constant stirring. Within 10 – 15 min the formation of products as orange solids was observed. After 3 h of refluxing the resulting mixture was diluted with water. The product was filtered, washed with water and dried. For removing the hydrophilic impurities, the product was dissolved in toluene and filtered through silica gel. The estimated yield was 80 – 90 %.

*Syn-5,10,15-triol-5,10,15-tribenzyl-10,15-dihydro-5H-diindeno[1,2-a;1′,2′-c]fluorene (**VIIa**)*

(0.28 g, 21 %). White solid. R_f = 0.27 (Et_2O/hexane, 1 : 1). – ^{1}H NMR ($CDCl_3$, 300 MHz): δ = 2.23 (s, 3H), 2.88 (d, J = 13.3 Hz, 3H), 3.34 (d, J = 13.3 Hz, 3H), 6.46 – 6.49 (m, 6H), 6.86 – 6.96 (m, 12H), 7.08 (t, J =7.2 Hz, 3H), 7.20 (t, J = 7.2 Hz, 3H), 8.37 (d, J = 7.7 Hz, 3H). – ^{13}C NMR ($CDCl_3$, 300 MHz): δ = 42.96, 83.00, 123.91, 125.97, 126.26, 127.22, 127.32, 128.86, 130.38, 135.94, 136.85, 137.04, 142.95, 148.32. – MALDI-TOF MS (DCTB/Ag-triflate): m/z = 767.2 $[M+Ag]^+$. – $C_{48}H_{36}O_3$: calcd. C 87.25, H 5.49; found C 87.16, H 5.50.

*Anti-5,10,15-triol-5,10,15-tribenzyl-10,15-dihydro-5H-diindeno[1,2-a;1′,2′-c]fluorene (**VIIb**)*

(0.43 g, 33 %). Cream solid. R_f = 0.61 (Et_2O/hexane, 1 : 1). – ^{1}H NMR ([D_6]-DMSO, 300 MHz): δ = 1.42 (d, J = 13.7 Hz, 1H), 2.15 (d, J = 13.2 Hz, 1H), 2.55 (d, J = 13.8 Hz, 1H), 2.73 (s, 2H), 2.98 (d, J = 13.2 Hz, 1H), 5.27 (s, 1H), 5.32 (s, 1H), 5.33 (s, 1H), 5.65 – 6.61 (m, 24H), 7.94 (d, J = 7.5 Hz, 1H), 8.05 (d, J = 7.7 Hz, 1H), 8.12 (d, J = 7.6 Hz, 1H). – ^{13}C NMR ([D_6]-DMSO, 300 MHz): δ = 42.52, 43.29, 44.30, 81.50, 82.24, 83.33, 123.76, 124.42, 124.66, 126.15, 126.18, 126.24, 126.36, 126.79, 126.92, 127.32, 127.90, 127.97, 128.03, 130.18, 130.79, 130.83, 35.93, 136.24, 136.33, 136.71, 136.77, 137.19, 137.63, 137.70, 138.34, 144.07, 144.19, 144.35, 149.49, 149.54, 149.58 (5 signals were not observed due to overlapping). – MALDI-TOF MS (DCTB/Ag-triflate): m/z = 767.2 $[M+Ag]^+$. – $C_{48}H_{36}O_3$: calcd. C 87.25, H 5.49; found C 86.98, H 5.54.

*5,10,15-Tribenzylidene-10,15-dihydro-5H-diindeno[1,2-a;1′,2′-c]fluorene (**VIIc**)*

Mixture of several *E/Z* isomers (286 mg, 72 %). Yellow solid. R_f = 0.31 (CH_2Cl_2/PE, 1 : 2). – ^{1}H NMR ($CDCl_3$, 300 MHz): δ = 6.58 – 7.74 (m, 27H), 8.47 – 8.59 (m, 3H). – MALDI-TOF MS (DCTB/Ag-triflate): m/z = 607.2 $[M+H]^+$, 713.1 $[M+Ag]^+$. – $C_{48}H_{30}$: calcd. C 95.02, H 4.98; found C 94.65, H 5.43.

*Syn-5,10,15-triol-5,10,15-tris-(4-bromo-benzyl)-10,15-dihydro-5H-diindeno[1,2-a;1′,2′-c]fluorene (**VIIIa**)*

(0.26 g, 14 %). White solid. R_f = 0.31 (Et_2O/PE, 1 : 1). – ^{1}H NMR ($CDCl_3$, 300 MHz): δ = 2.20 (s, 3H), 2.75 (d, J = 13.3 Hz, 3H), 3.30 (d, J = 13.3 Hz, 3H), 6.28 – 6.44 (m, 6H), 6.85 – 7.49 (m, 12H), 8.32 (d, J = 7,6Hz, 3H). – ^{13}C NMR ($CDCl_3$, 300 MHz): δ = 42.49, 82.70, 120.49, 123.87, 125.95, 127.66, 129.21, 130.39, 132.03, 134.79, 136.75, 136.83, 142.80, 147.95. – MALDI-TOF MS (DCTB/Ag-triflate): m/z = 1000.9 $[M+Ag]^+$. – $C_{48}H_{33}Br_3O_3$: calcd. C 64.24, H 3.71; found C 64.18, H 4.22.

*Anti-5,10,15-triol-5,10,15-tris-(4-bromo-benzyl)-10,15-dihydro-5H-diindeno[1,2-a;1′,2′-c]fluorene (**VIIIb**)*

(0.41 g, 23 %). White solid. R_f = 0.67 (Et_2O/PE, 1 : 1). – ^{1}H NMR ($CDCl_3$, 300 MHz): δ = 2.14 – 3.66 (m, 9H), 6.43 (d, J = 8.3, 2H), 6.49 (d, J = 8.3 Hz, 2H), 6.68 (d, J = 8.3 Hz, 2H), 7.00 – 7.47 (m, 15H), 8.71 – 8.74 (m, 3H). – ^{13}C NMR ($CDCl_3$, 300 MHz): δ = 42.04, 42.81, 43.26,

82.66, 83.42, 83.88, 120.39, 120.53, 123.17, 123.83, 123.93, 124.35, 126.31, 126.39, 126.53, 127.60, 127.70, 127.93, 129.30, 130.23, 130.35, 130.50, 131.94, 132.06, 132.40, 134.77, 135.22, 137.03, 137.13, 137.79, 141.82, 142.48, 142.93, 148.27, 148.49, 148.64 (6 signals were not observed due to overlapping). – MALDI-TOF MS (DCTB/Ag-triflate): *m/z* = 1000.9 $[M+Ag]^+$. – $C_{48}H_{33}Br_3O_3$: calcd. C 64.24, H 3.71; found C 63.18, H 4.92.

*5,10,15-Tris-(4-bromo-benzylidene)-10,15-dihydro-5H-diindeno[1,2-a;1′,2′-c]fluorene (**VIIIc**)*

Mixture of several *E/Z* isomers (201 mg, 82 %). Yellow solid. R_f = 0.49 (CH_2Cl_2/PE, 1 : 2). – ^{1}H NMR ($CDCl_3$, 300 MHz): δ = 6.6 – 7.7 (m, 24H), 8.3 – 8.6 (m, 3H). – MALDI-TOF MS (DCTB/Ag-triflate): *m/z* = 841.0 $[M+H]^+$, 946.9 $[M+Ag]^+$. – $C_{48}H_{27}Br_3$: calcd. C 68.35, H 3.23; found C 68.81, H 3.43.

*Syn-5,10,15-triol-3,8,13-tribromo-5,10,15-tribenzyl-10,15-dihydro-5H-diindeno[1,2-a;1′,2′-c]fluorene (**IXa**)*

(33 mg, 12 %). Yellowish solid. R_f = 0.59 (Et_2O/PE, 1 : 1). – ^{1}H NMR ($CDCl_3$, 300 MHz): δ = 2.55 (d, *J* = 13.3 Hz, 3H), 3.18 – 3.27 (m, 6H), 6.60 – 6.67 (m, 6H), 6.72 (d, *J* = 8.0 Hz, 3H), 7.00 – 7.38 (m, 12H), 8.49 (s, 3H). – ^{13}C NMR ($CDCl_3$, 300 MHz): δ = 43.77, 82.60, 123.08, 124.92, 126.83, 127.70, 128.86, 130.51, 130.60, 135.05, 135.62, 138.48, 143.93, 146.47. – MALDI-TOF MS (DCTB/Ag-triflate): *m/z* = 1000.7 $[M+Ag]^+$.

*Anti-5,10,15-triol-3,8,13-tribromo-5,10,15-tribenzyl-10,15-dihydro-5H-diindeno[1,2-a;1′,2′-c]fluorene (**IXb**)*

(102 mg, 38 %). Cream solid. R_f = 0.78 (Et_2O/PE, 1 : 1). – ^{1}H NMR ([D$_6$]-DMSO, 300 MHz): δ = 2,15 (d, *J* = 13.8 Hz, 1H), 2.94 (d, *J* = 13.8 Hz, 1H), 3.22 (d, *J* = 13.8, 1H), 3.30 (s, 3H), 3.38 – 3.51 (m, 2H), 3.70 (d, *J* = 13.8 Hz, 1H), 6.37 (s, 1H), 6.43 – 6.48 (m, 4H), 6.64 (d, *J* = 8.0, 1H), 6.80 – 6.93 (m, 6H), 6.99 (d, *J* = 8.0, 1H), 7.06 – 7.21 (m, 5H), 7.06 – 7.21 (m, 3H), 8.93 (s, 1H), 9.02 (s, 1H), 9.12 (s, 1H). – ^{13}C NMR ([D$_6$]-DMSO, 300 MHz): δ = 40.5, 41.09, 42.20, 79.20, 80.00, 81.19, 119.14, 119.37, 119.41, 123.83, 123.99, 124.34, 124.48, 124.55, 125.15, 125.52, 125.58, 126.75, 127.03, 127.11, 127.29, 127.70, 128.11, 128.67, 128.75, 132.76, 133.22, 133.45, 133.55, 133.99, 134.44, 137.43, 137.56, 138.15, 143.11, 143.34, 143.43, 146.37, 146.46, 146.48 (2 signals were not observed due to overlapping). – MALDI-TOF MS (DCTB/Ag-triflate): *m/z* = 1000.8 $[M+Ag]^+$.

*5,10,15-Tribenzylidene-3,8,13-tribromo-10,15-dihydro-5H-diindeno[1,2-a;1′,2′-c]fluorene (**IXc**)*

Mixture of several *E/Z* isomers (68 mg, 90 %). Yellow solid. R_f = 0.31 (CH_2Cl_2/PE, 1 : 2). – ^{1}H NMR ($CDCl_3$, 300 MHz): δ = 6.85 – 7.8 (m, 24H), 8.35 – 8.75 (m, 3H). – MALDI-TOF MS (DCTB/Ag-triflate): *m/z* = 946.6 $[M+Ag]^+$.

*Syn-5,10,15-triol-5,10,15-tris-naphthalen-2-ylmethyl-10,15-dihydro-5H-diindeno[1,2-a;1′,2′-c]fluorene (**Xa**)*

(0.38 g, 23 %). Cream solid. R_f = 0.26 (Et_2O/hexane, 1 : 1). – ^{1}H NMR ($CDCl_3$, 300 MHz): δ = 2.32 (s, 3H), 2.62 (d, *J* = 13.4Hz, 3H), 3.41 (d, *J* = 13.4Hz, 3H), 6.67 – 6.72 (m, 6H), 6.99 – 7.04 (m, 6H), 7.14 – 7.56 (m, 15H), 7.80 – 7.84 (m, 3H), 8.47 (d, *J* = 7,7 Hz, 3H). – ^{13}C NMR ($CDCl_3$, 300 MHz): δ = 43.22, 83.05, 123.98, 125.21, 125.52, 125.89, 126.43, 127.24, 127.38, 127.87, 128.34, 128.95, 129.17, 132.08, 132.75, 132.82, 136.52, 137.12, 143.50, 148.19. – MALDI-TOF MS (DCTB/Ag-triflate): *m/z* = 917.2 $[M+Ag]^+$. – $C_{60}H_{42}O_3$: calcd. C 88.86, H 5.22; found C 88.58, H 5.31.

*Anti-5,10,15-triol-5,10,15-tris-naphthalen-2-ylmethyl-10,15-dihydro-5H-diindeno[1,2-a;1′,2′-c]fluorene (**Xb**)*

(0.42 g, 26 %). Yellowish solid. R_f = 0.45 (Et_2O/hexane, 1 : 1). – ^{1}H NMR ($CDCl_3$, 300 MHz): δ = 2.03 (s, 1H), 2.35 (s, 1H), 2.39 (s, 1H), 2.56 (d, *J* = 13.7 Hz, 1H), 3.42 (d, *J* = 13.7 Hz, 1H), 3.43 (d, *J* = 13.5 Hz, 1H), 3.46 (d, *J* = 13.7 Hz, 1H), 3.87 (d, *J* = 13.0 Hz, 1H), 3.88 (d, *J* = 13.0 Hz, 1H), 6.80 – 7.68 (m, 30H), 8.74 (d, *J* = 7.8 Hz, 1H), 8.82 (d, *J* = 7.8 Hz, 1H), 8.86 (d, *J* = 7.7 Hz, 1H). – ^{13}C NMR ($CDCl_3$, 300 MHz): δ = 42.54, 43.55, 43.86, 83.12, 83.82, 84.12, 124.01, 124.35, 125.28, 125.51, 125.57, 126.32, 126.40, 126.47, 126.51, 126.56, 127.36, 127.39, 127.42, 127.46, 127.51, 127.57, 128.93, 129.05, 129.07, 129.17, 129.21, 129.26, 132.09, 132.14, 132.79, 132.83, 132.86, 133.59, 133.62, 133.98, 137.33, 137.39, 137.62, 137.87, 142.30, 142.72, 143.57, 148.62, 148.78, 148.97 (14 signals were not observed due to overlapping). – MALDI-TOF MS (DCTB/Ag-triflate): *m/z* = 917.2 $[M+Ag]^+$. – $C_{60}H_{42}O_3$: calcd. C 88.86, H 5.22; found C 87.71, H 5.62.

*5,10,15-Tris-naphthalen-2-ylmethylene-10,15-dihydro-5H-diindeno[1,2-a;1′,2′-c]fluorene (**Xc**)*

Mixture of several *E/Z* isomers (336 mg, 86 %). Yellow solid. R_f = 0.73 (CH_2Cl_2/PE, 1 : 1). – ^{1}H NMR ($CDCl_3$, 300 MHz): δ = 6.5 – 7.8 (m, 33H), 8.4 – 8.7 (m, 3H). – MALDI-TOF MS (DCTB/Ag-triflate): *m/z* = 757.3 $[M+H]^+$, 863.2 $[M+Ag]^+$. – $C_{60}H_{36}$: calcd. C 95.21, H 4.79; found C 93.72, H 4.64.

*Syn-5,10,15-triol-3,8,13-tribromo-5,10,15-tris-naphthalen-2-ylmethyl-10,15-dihydro-5H-diindeno[1,2-a;1′,2′-c] fluorene (**XIa**)*

(82 mg, 26 %). Cream solid. R_f = 0.39 (Et_2O/hexane, 1 : 1). – ^{1}H NMR ($CDCl_3$, 300 MHz): δ = 2.38 (d, *J* = 13.5 Hz, 3H), 3.20 (d, *J* = 13.5 Hz, 3H), 3.37 (s, 3H), 6.67 (d,

J = 8.0 Hz, 3H), 6.77 (d, J = 8.0 Hz, 3H), 7.06 (s, 3H), 7.2 – 7.7 (m, 6H), 8.54 (s, 3H). – ^{13}C NMR ($CDCl_3$, 300 MHz): δ = 43.95, 82.60, 123.08, 124.87, 125.66, 125.94, 127.03, 127.42, 127.45, 128.78, 128.96, 129.30, 130.61, 132.28, 132.60, 132.80, 135.54, 138.51, 144.11, 146.53. – MALDI-TOF MS (DCTB/Ag-triflate): m/z = 1151.0 $[M+Ag]^+$.

*Anti-5,10,15-triol-3,8,13-tribromo-5,10,15-tris-naphthalen-2-ylmethyl-10,15-dihydro-5H-diindeno[1,2-a;1′,2′-c] fluorene (**XIb**)*

(66 mg, 21 %). Cream solid. R_f = 0.56 (Et_2O/hexane, 1 : 1). – ^{1}H NMR ($CDCl_3$, 300 MHz): δ = 2.14 (s, 1H), 2.34 (s, 1H), 2.38 (s, 1H), 2.48 (d, J = 13.4 Hz, 1H), 3.14 (d, J = 13.2 Hz, 1H), 3.33 (d, J = 13.2 Hz, 1H), 3.41 (d, J = 13.4 Hz, 1H), 3.80 – 3.95 (m, 2H), 6.80 (d, J = 8.0 Hz, 1H), 6.85 – 7.80 (m, 26H), 8.99 (s, 1H), 9.01 (s, 1H), 9.10 (s, 1H). – ^{13}C NMR ($CDCl_3$, 300 MHz): δ = 42.62, 43.48, 44.00, 82.64, 83.21, 83.79, 123.22, 123.28, 123.33, 125.52, 125.60, 125.64, 125.83, 125.85, 125.87, 126.90, 127.02, 127.40, 127.48, 127.53, 127.61, 128.82, 128.93, 129.00, 129.41, 129.49, 129.63, 129.74, 132.21, 132.25, 132.75, 132.82, 132.84, 132.88, 132.90, 133.10, 136.21, 136.30, 136.45, 138.77, 138.97, 139.45, 143.62, 143.77, 144.81, 147.25, 147.33, 147.51 (12 signals were not observed due to overlapping). – MALDI-TOF MS (DCTB/Ag-triflate): m/z = 1151.0 $[M+Ag]^+$.

*3,8,13-Tribromo-5,10,15-tris-naphthalen-2-ylmethylene-10,15-dihydro-5H-diindeno[1,2-a;1′,2′-c] fluorene (**XIc**)*

Mixture of several *E/Z* isomers (67 mg, 88 %). Orange solid. R_f = 0.21 (CH_2Cl_2/PE, 1 : 2). – ^{1}H NMR ($CDCl_3$, 300 MHz): δ = 6.4 – 8.0 (m, 30H), 8.3 – 8.7 (m, 3H). – MALDI-TOF MS (DCTB/Ag-triflate): m/z = 1096.88 $[M+Ag]^+$.

[1] L. T. Scott, *Angew. Chem. Int. Ed*. **2004**, *43*, 4994 – 5007.
[2] G. Mehta, S. R. Rao, *Tetrahedron* **1998**, *54*, 13325 – 13370.
[3] L. T. Scott, *Pure Appl. Chem*. **1996**, *68*, 291 – 300.
[4] V. M. Tsefrikas, L. T. Scott, *Chem. Rev*. **2006**, *106*, 4868 – 4884.
[5] M. Szwarc, D. Williams, *J. Chem. Phys*. **1952**, *20*, 1171 – 1172.
[6] M. Ladaki, M. Szwarc, *J. Chem. Phys*. **1952**, *20*, 1814 – 1816.
[7] M. A. Brooks, L. T. Scott, *J. Am. Chem. Soc*. **1999**, *121*, 5444 – 5449.
[8] S. Hagen, M. S. Bratcher, M. S. Erickson, G. Zimmermann, L. T. Scott, *Angew. Chem. Int. Ed*. **1997**, *36*, 406 – 408.
[9] R. Faust, K. P. C. Vollhardt, *Abstracts of Papers*, abstract N61, 7th International Symposium on Novel Aromatic Compounds, Victoria, British Columbia (Canada) **1992**.
[10] L. T. Scott, M. M. Boorum, B. J. McMahon, S. Hagen, J. Mack, J. Blank, H. Wegner, A. de Meijere, *Science* **2002**, *295*, 1500 – 1503.
[11] M. M. Boorum, Y. V. Vasil'ev, T. Drewello, L. T. Scott, *Science* **2001**, *294*, 828 – 831.
[12] G. Mehta, P. V. V. S. Sarma, *Tetrahedron Lett*. **2002**, *43*, 9343 – 9346.
[13] B. Gomez-Lor, O. de Frutos, A. M. Echavarren, *Chem. Commun*. **1999**, 2431 – 2432.
[14] M. J. Plater, *J. Chem. Soc., Perkin Trans. 1* **1997**, 2897 – 2901.
[15] A. H. Abdourayak, Y. Marcinow, A. Sygula, R. Sygula, P. W. Rabideau, *J. Am. Chem. Soc*. **1995**, *117*, 6410 – 6411.
[16] F. Sbrogio, F. Fabris, O. De Lucchi, *Synlett* **1994**, 761 – 762.
[17] E. V. Dehmlow, T. Kelle, *Syn. Commun*. **1997**, *27*, 2021 – 2031.
[18] M. J. Plater, M. Praveen, A. R. Howie, *J. Chem. Res. (S)* **1997**, 46 – 47.
[19] M. D. Golden, S. W. Benson, *Chem. Rev*. **1969**, *69*, 125 – 134.
[20] B. Gomez-Lor, C. Koper, R. H. Fokkens, E. J. Vlietstra, T. J. Cleij, L. W. Jenneskens, N. M. M. Nibbering, A. M. Echavarren, *Chem. Commun*. **2002**, *4*, 370 – 371.
[21] Y. Rubin, *Chem. Eur. J*. **1997**, *3*, 1009 – 1016.
[22] J. Osterodt, A. Zett, F. Vögtle, *Tetrahedron* **1996**, *52*, 4949 – 4962.
[23] M. J. Frisch, G. W. Trucks, H. B. Schlegel, G. E. Scuseria, M. A. Robb, J. R. Cheeseman, V. G. Zakrzewski, J. A. Montgomery, Jr., R. E. Stratmann, J. C. Burant, S. Dapprich, J. M. Millam, A. D. Daniels, K. N. Kudin, M. C. Strain, O. Farkas, J. Tomasi, V. Barone, M. Cossi, R. Cammi, B. Mennucci, C. Pomelli, C. Adamo, S. Clifford, J. Ochterski, G. A. Petersson, P. Y. Ayala, Q. Cui, K. Morokuma, D. K. Malick, A. D. Rabuck, K. Raghavachari, J. B. Foresman, J. Cioslowski, J. V. Ortiz, A. G. Baboul, B. B. Stefanov, G. Liu, A. Liashenko, P. Piskorz, I. Komaromi, R. Gomperts, R. L. Martin, D. J. Fox, T. Keith, M. A. Al-Laham, C. Y. Peng, A. Nanayakkara, M. Challacombe, P. M. W. Gill, B. Johnson, W. Chen, M. W. Wong, J. L. Andres, C. Gonzalez, M. Head-Gordon, E. S. Replogle, J. A. Pople, GAUSSIAN 03, revision C.02, Gaussian, Inc., Wallingford CT (USA) **2004**.
[24] C. Lambert, G. Nöll, E. Schmälzlin, K. Meerholz, C. Bräuchle, *Chem. Eur. J*. **1998**, *4*, 2129 – 2135.
[25] K. Yu. Amsharov, K. Simeonov, M. Jansen, *Carbon* **2007**, *45*, 337 – 343.